Experimental Evaluations of Model Piles Subject to Inclined Loading in Sand

Nabaa A. Al-Fahham[1*],,and *Ali* A. Al-Jazaairry

[1] Civil Engineering Department, University of Kufa, Najaf, Iraq.

Abstract. The structures that subjected to varying loads are supported by pile foundations. These loads consist of inclined and vertical loads. The main objective of this work is to experimentally investigate the effects of an inclined load on the lateral pile reaction and axial pile displacement for piles found in cohesionless soil. For this purpose, the slenderness ratios of model steel piles are varied by values of 11, 14, and 17. Moreover, the pile shapes involved in this study are H-pile, closed end circular and square. The experimental tests were conducted in sandy soil. However, the load inclination angle included in assessing the pile behavior were 0, 30, 45, and 60 from the vertical. In order to study the above parameters on the behavior of model pile, thirty-six experimental tests were carried out. Several findings indicated that the lateral pile deflection was highly influenced by increasing the load inclination. Further, the load inclination effect on the pile's ultimate bearing capacity is high which leads to a reduction in the pile's capacity. Additionally, the vertical displacement of pile is less than horizontal displacement when the pile is subjected to an inclined load of 45° and the model fails by horizontal displacement.

1 INTRODUCTION

Many structures' foundations must withstand inclined compressive loads, such as those of offshore structures, transmission towers, and wind energy converter towers. In such situations, piles may be used to reduce the corresponding settlements and raise the adopted foundations' load carrying capacities. The behaviour of rigid piles under inclined loads in uniform soils has been extensively studied by means of instrumented model pile tests [1-6]. (Poulos and Davis ,1980) [7] stated that the ultimate load capacity can be used to determine the failure of a vertical pile under inclined loads. Meyerhof and his co-workers [3-6] conducted an extensive study on the behaviour of rigid piles embedded in both homogeneous and layered soils, subjected to inclined loads. The study was based on the experimental results from numerous loading tests conducted on small-scale piles. Large inclinations will lead to lateral failure as the load approaches perpendicular to the pile axis, while small deviations in the used load's direction from the axial direction will primarily result in axial slip. (Meyerhof and Ranjan, 1972) [8] stated that in compact and dense sand, the ultimate loads for vertical piles decrease with an increase in the inclination of the load with the vertical, according to experimental findings and field tests. (Conte et al., 2021) [9] discovered that the applied load's inclination has a major impact on the piles' bearing capacity. It is discovered that the pile's ultimate bearing capacity falls with increasing load inclination. This is because the pile's effective area, which is able to withstand an inclined load, has decreased. Argues that in order to guarantee pile stability and avoid failure, the inclination angle should be taken into account during the design process. According to (Chirlam Charla, 2021) [10] there was a significant decrease in the lateral deflection of piles and pile groups with an increase in the vertical deformation that accompanied the increase in load inclination. (Kalthiya et al., 2021) [11] discovered a direct relationship between decreased bearing capacities and an increase in the load inclination angle. Furthermore, the pile's bearing capacities rise with an increase in the slenderness ratio.

* *Corresponding author:* alia.aljazairi@uokufa.edu.iq

2 SOIL PROPERTIES

The sandy soil used in this study was taken from the middle of the Iraqi specifically from Najaf city. Several chemical analyses were conducted on the soil, such as the T.D.S. test, gypsum concentration, sulfate content (SO_4), and soil organic content, as indicated in Table 1. However, it is important to note that this study's tests were conducted in the Department of Civil Engineering Laboratory at the University of Kufa.

TABLE 1. Characteristic properties of reclaimed soil

Soil property	Value	Specification
T.D.S (Total Dissolved Solids)	0.74 %	B.S 1337 PART.3
Gypsum content	4.75 %	
SO_4	2.21 %	
Organic materials	0.35 %	

Additionally, a number of tests were used to physically examine the soil, including the Proctor test, minimum dry unit weight, specific gravity, optimal moisture content (O.M.C.), sieve analysis (Figure 1), field unit weight, and direct shear test. The physical characteristics of the utilized soil is shown in Table 2.

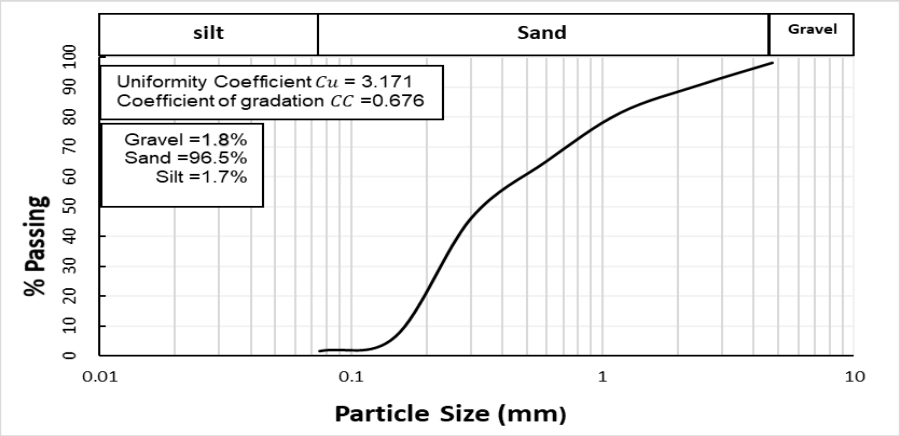

Fig 1. The grain size distribution curve of used soil

TABLE 2. Physical characteristics of the utilized soil

Soil Property	Value	Specification
Water Content of site Soil (%)	5	ASTM D 2216 – 10 [12]
Field unit weight (kN/m^3)	17.5	ASTM D 1556-07 [13]
D_{10}, (mm)	0.16	ASTM D 422-63 [14]
D_{30}, (mm)	0.24	

D_{60}, (mm)	0.52	
Coefficient of uniformity (Cu)	3.2	-
Coefficient of curvature (Cc)	0.68	-
Soil Classification	SP	Unified Soil Classification system (USCS)
Maximum dry unit weight (Procter) (kN/m^3)	18.48	ASTM D 698-07 [15]
Optimum moisture content (O.M.C), (%)	12	
Friction angle, Ø (°)	37	ASTM D 3080-7 [16]
Cohesion (kN/m^2)	4.85	
Minimum dry unit weight (kN/m^3)	15.6	ASTM D 4254-16 [17]
Specific Gravity Gs	2.67	ASTM D 854 [18]
Relative density, Dr (%)	40	-

3 TESTING APPARATUS

3.1 The Loading System

The metal frame is constructed from two 3.5-inch channel plates that are 1.5 meters long (measured from the bottom of the box to the upper end). These plates are installed on the box's sides. The side channel plates, which each have 19 mm holes and a 50 mm space between them, can be slid to move the main channel plate vertically up and down as needed. The upper plate is also a channel plate with a length of 850 mm. The two ends are closed with 19 mm holes so that they can be installed using the previously mentioned holes and 19 mm stainless steel bolts. The base of an electric jack is composed of two metal plates that have a combined thickness of 6 mm. The metal plates are attached to a metal tube that has a diameter of 30.2 mm. The top plate has holes in it so that it can be fixed to another plate that is perforated and placed on top of the frame's upper channel plate. To secure the jack inside the base, the bottom plate is perforated. Figure 2 shows the loading frame and the stainless steel bolts with a diameter of 19 mm and a length of 100 mm are used to secure it to the base.

Fig 2. Loading unit

3.2 Pile Model

There were three different kinds of steel model piles used: close-ended square piles, close-ended circular piles, and H-piles. Every pile has the exact same 25 mm width. In addition, three length-to-diameter ratios (L/D) of 11, 14, and 17 have been utilized to characterize the pile lengths. The study aims to comprehend the effects of model pile shapes on pile-bearing capacity. To avoid boundary and scale effects in the current experimental study, the model pile diameter was selected based on recommendations from [19]. One rule is that when performing the model pile capacity estimation tests, the ratio of the container diameter to the pile diameter (D container/D pile) must be greater than 8 in order to eliminate the wall effects [20].

3.3 Testing Box

A 700 x 700 mm steel container with a 2 mm thick steel plate was employed. In order to eliminate the influence of boundary conditions in the model tests, these dimensions were chosen. According to (Poulos and Davis, 1980) [7], the area impacted by driving a pile in cohesionless soil ranges from 4.5 and 5.5 times the diameter from the pile's side. Nonetheless, the current study's pile-to-container wall distance is 14 times greater than the pile diameter, which is obviously higher than the advised ratio. The steel container arrived 800 mm high. The driving pile's influence in the cohesiveness soil should be three to four times its diameter below the pile tip, based on previous studies, [7]. This guideline informed the choice of depth. To ensure that the required soil density was reached during the soil filling process, the box was divided into eight equal parts from the inside using clear lines.

3.4 Sand Density Control Technique

The density needed for the test, or the density used during the testing procedure that is same to the natural field density of 17.5 kN/m^3, determines how much soil is needed for each layer. Prior to compacting the soil in the box, the water content of the soil is measured using a microwave after the weight of soil required for each layer has been determined. As per ASTM D-4643 [21] guidelines, three samples are obtained for every stratum, and each sample's water content is checked. Soil is added to fill a layer once the water content has been verified. To make the strata easy to distinguish, lines are used to divide the interior side of the soil box. After adding the soil for each layer, the surface needs to be leveled and compacted to the necessary density.

4 The Measuring System

The loading system consists of a screw hydraulic jack with a maximum load capacity of 500 kg that is connected to a control system for jack control. By controlling the jack's movement as well as the loading's direction, this technique permits compressive loading to be that applies to the pile. The jack is fastened to a tiny motor in order to supply steady electricity while applying the load. A voltage regulator that powers a small motor is wired to a power source, and it remains constant during the test. The jack's end is secured with a bolt measuring 18 mm in diameter and 110 mm in length. The load cell is attached to the second side of this bolt in order to record the applied load. Two Differential Linear Variable Transformer (LVDTs) were used to measure the movements of the pile. All of the readings from the load cell and LVDTs were also recorded and stored using a data collection program called LabVIEW. National Instruments offers a visual programming language and development environment called LabVIEW. The definition of LabVIEW is provided by a Laboratory Virtual Instrumentation Engineering Workbench. The devices were calibrated prior to the tests, and the data was sent as tables for the computer to process. Figure 3 displays a schematic diagram of a testing system.

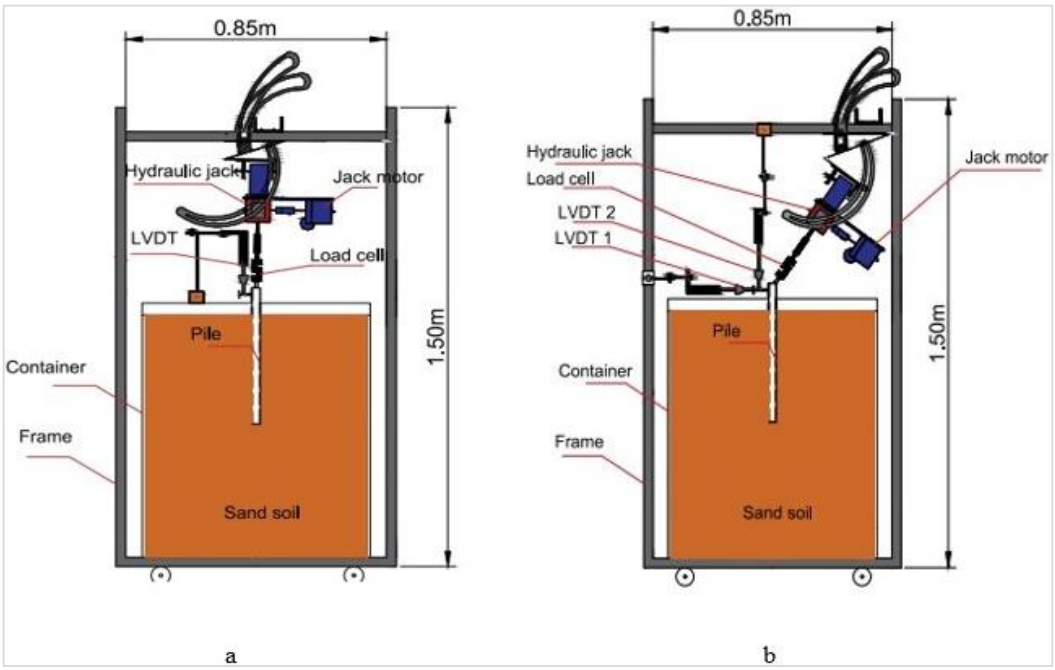

Fig. 3. The testing system's schematic diagram

5 EXPERIMENTAL PROGRAM

5.1 Preparing the Soil and Installing the Model Pile

To reach the necessary soil unit weight of 17.5 kN/m^3, the soil is prepared. next choosing the pile model to be tested, taking into account its type and slenderness ratio. The temporary pile holder installs the model pile, and in layers of sand, the soil is poured into the container until the top. The loading head is then placed on the pile after the pile holder is removed, the LVDTs are installed. This process was repeated for all piles included the current research work.

5.2 Pile Testing

The testing frame is fixed to the loading system. Next, using a hydraulic jack to gradually apply a vertical or inclined compression force, the LVDTs are installed to measure the horizontal and vertical displacements. Then, they record the pile's displacements on the data recorder after the load is applied. Figure 4 shows how the pile is loaded.

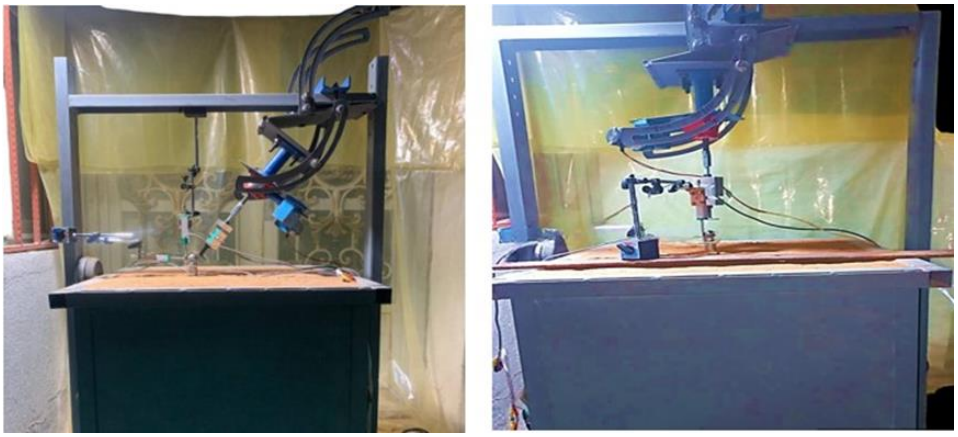

FIGURE 4. Testing of the pile

6 EXPERIMENTAL RESULTS AND DISCUSSION

Thirty-six loading (vertical and incline) tests were conducted for three slenderness ratios and three pile shape in order to assess the pile's bearing capacity. A load cell had recorded the applied load on the pile during the tests, and two LVDTs had recorded the pile's movement (both vertically and horizontally). The bearing capacity of pile (Qu) and failure resistance of the pile are impacted by these factors. The study's parameters include the pile's shape, length, and the load inclination angle with the vertical axis (α), which are all produced by the load. The variations in the pile's displacement with the load generated for each testing condition are displayed in the following sections. The behavior of the nonlinear load-displacement curves is comparable. By using of load versus displacement graphs, the effects of pile length, pile shape, and load direction were investigated. The ultimate load capacity of the piles was ascertained by measuring the load at which the load-displacement graph's curve peaks or at which the load moves continuously [22].

7 EFFECT OF PILE SHAPE

7.1 Vertical Loading Test

Before starting the considering tests to extract the research data, a number of experimental tests were carried out to ensure the accuracy of the results and the loading system. The load settlement curve is used to calculate the load at failures in all model tests of pile shapes. An alternative way to define a failure load is the abscissa of the point on the load-settlement curve where the start and final tangents intersect (Method of Tangent) [23].

Ultimate Pile Capacity for L/D ratio=11

A static load test was utilized to ascertain the ultimate bearing capacity (Qu) of the piles. The load-settlement curves for each type of pile are displayed in Figure 5. The carrying capacity of the closed-ended square pile is higher than that of the closed-ended circular and H-pile, by 8% and 24%, respectively.

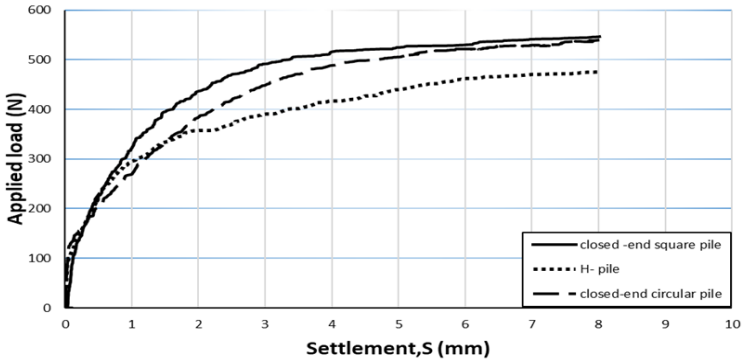

Fig. 5. Load-settlement curves for various pile shapes with L/D = 11.

The closed-end square pile had a relatively high pile bearing capacity (Qu) through the test procedure because of its larger end bearing point and surface area when compared to other pile shapes. The piles that follow are closed-end circular piles. Comparing the H pile to the other piles in this test, it was found that the pile load capacity was the lowest. This is shown by the formal settlement.

Ultimate Pile Capacity for L/D ratio=14

The load settlement curves for different pile shapes were displayed in Figure 6. Settlements in H-piles were evidently valued higher than settlements in other pile shapes. The results showed that comparing to the close-ended circular pile and H- pile, the close-ended square pile's bearing capacity values increased by 17.33% and 46.67%, respectively. The piles' surface area and bearing capacity increase as they descend deeper and encounter stronger soil layers. Skin friction consequently risen, with the close-ended square pile (Qu) exhibiting a higher value than the other piles.

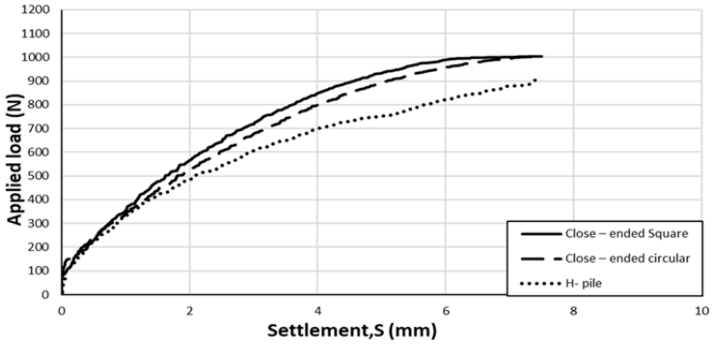

Fig 6. load settlement curves with L/D = 14 for different types of piles.

Ultimate Pile Capacity for L/D ratio=17

With different pile shapes embedded in sand soil, Figure 7 shows the applied load versus the pile settlement. The close-ended square pile has proven to be more resilient. By contrast, there was minimal resistance from the H-pile. However, since its value increases significantly with an increase in the embedment ratio in the sandy soil, comparing the close-end square pile to the other tested piles showed that it had a higher value of bearing capacity. This rise is the result of increasing the area in contact with the soil.

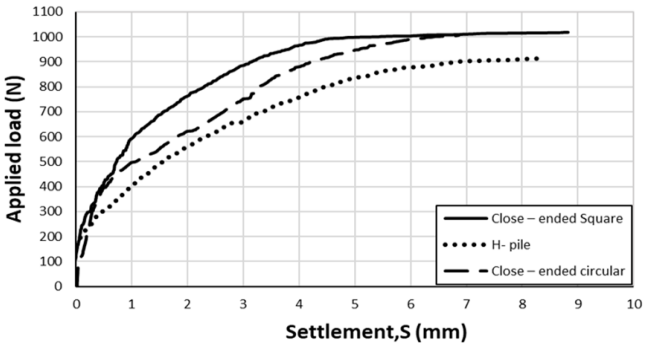

Fig. 7. Load-settlement curves with different pile shapes at L/D = 17.

A summary of the bearing capacity (Qu) of piles subject to vertical loads outcomes is given in Table 3.

TABLE 3. Pile bearing capacity of vertical loading test

L/D	Shapes	Qu (N)
11	H – Pile	420
	Close – ended circular	480
	Close – ended Square	520
14	H – Pile	600
	Close – ended circular	750
	Close – ended Square	880
17	H - Pile	800
	Close – ended circular	880
	Close – ended Square	1000

Inclined Load Tests at α=30°

In all searches involving piles, when an inclined load is applied at α=30°, the pile fails to settle laterally first, but its vertical displacement is nearly equal to its horizontal displacement.

Ultimate Pile Capacity for L/D ratio=11

The load-settlement curves for different pile shapes are shown in Figures 8 and 9. It is evident that compared to other pile shapes, close-ended square piles have greater capacity values. Comparing the close-ended square pile (Qu) to the close-ended circular and H-piles, the results show that the Qu values grew by 13.64% and 25%, respectively. The square pile's bearing capacity increases with its larger end bearing point.

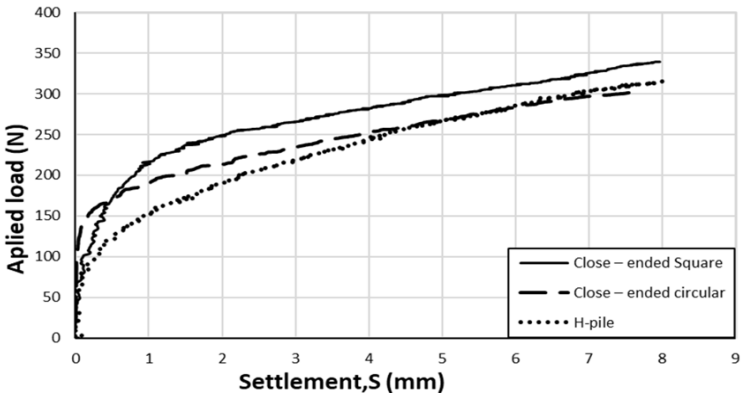

Fig 8. Load-horizontal settlement curves for different pile shapes with L/D = 11.

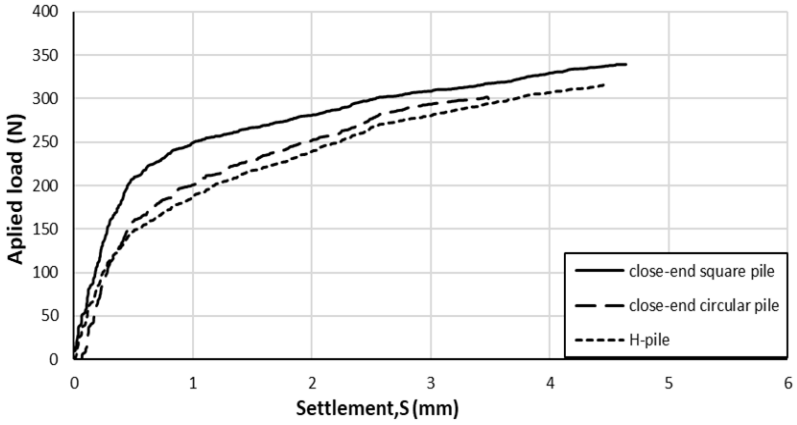

Fig 9. Load-vertical settlement curves for different pile shapes with L/D = 11.

Ultimate Pile Capacity for L/D ratio=14

Figures 10 and 11 show the relationships between applied load and settlement. The shape of the pile had a major impact on the increase in settlement. The close-ended square pile had the greatest bearing capacity, while the H-pile had a minimum value. The results indicate that the close-ended square pile (Qu) values are rose by 17.24% and 25.9%, when compared to the close-ended circular and H- piles respectively.

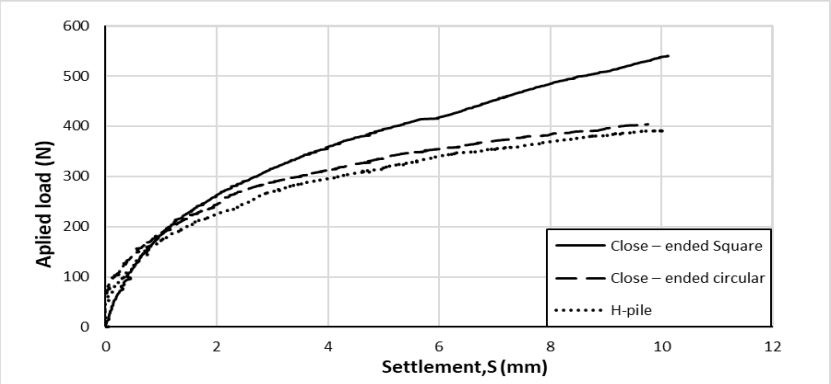

Fig 10. Load - horizontal settlement curves for different pile shapes with L/D = 14.

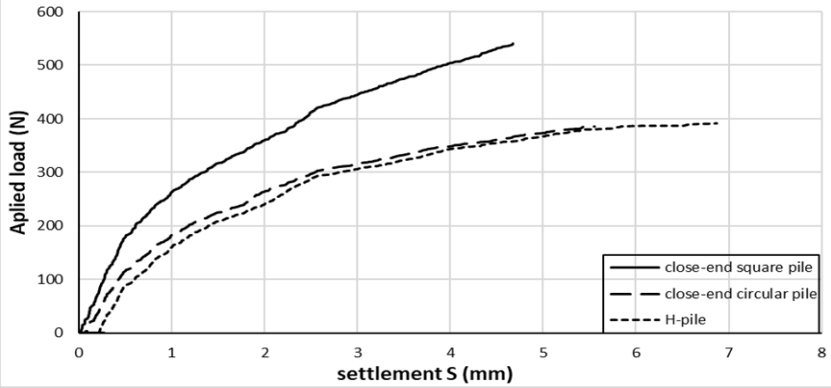

Fig 11. Load – vertical settlement curves for different pile shapes with L/D = 14.

Ultimate Pile Capacity for L/D ratio=17

The bearing capacity of pile is found for various types of piles as shown in Figures 12 and 13. It can be realized that all of the H-piles showed less resistance and more lateral settlement. The test results are shown in Table 8. It can be found that the values of Qu for close-ended square piles increased by 34.48% when compared to H-piles and by 25.81% when compared to the close-ended circular pile.

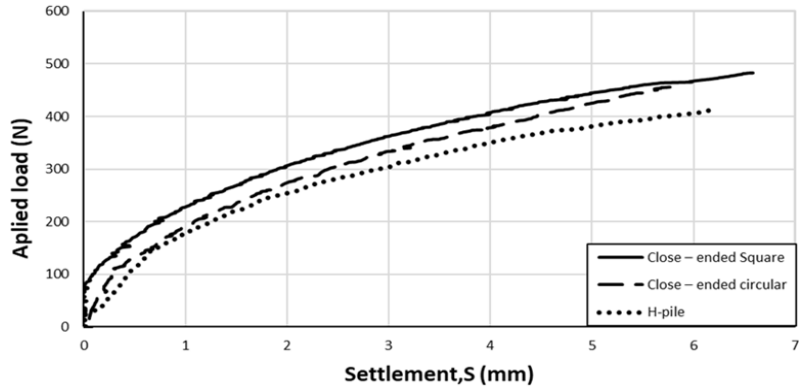

Fig. 12. Load - horizontal settlement curves for different pile shapes with L/D = 17.

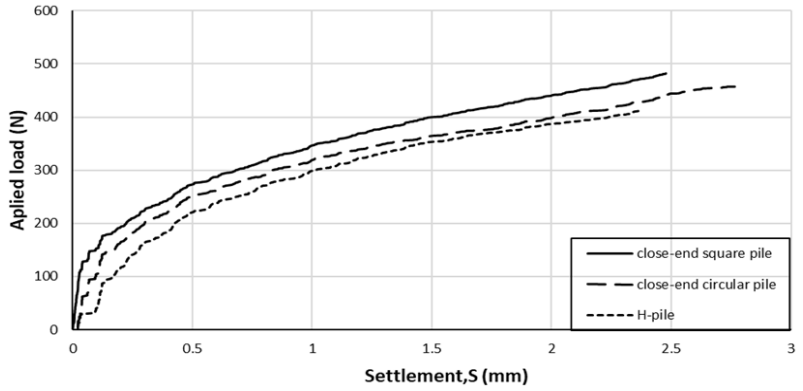

Fig 13. Load –vertical settlement curves for different pile shapes with L/D = 17.

Table 4 summarizes the results of the bearing capacity of piles subjected to inclined loads α=30°and horizontal settlement.

TABLE 4. The pile's bearing capacity at inclined load tests α=30°

L/D	Shapes	Qu Horizontal (N)	Qu Vertical (N)
11	Close – ended Square	250	270
	Close – ended circular	220	245
	H-pile	200	230
14	Close – ended Square	340	360
	Close – ended circular	290	320
	H-pile	270	300
17	Close – ended Square	390	410
	Close – ended circular	310	340
	H-pile	290	305

Inclined Load Tests at α=45°

All types of piles utilized in the current research showed vertical displacement is less than horizontal displacement when the pile is subjected to an inclined load at α=45°, and the model fails by horizontal displacement.

Ultimate Pile Capacity for L/D ratio=11

Figure 14 displays the load settlement curves for different pile forms when 45° inclined load with the vertical was used to determine the values of pile's bearing capacity. All piles fail in horizontal displacement. It is apparent that displacements in H-piles were valued more highly than displacements in other types of piles. The findings demonstrated that the close-ended square pile (Qu) values increased by 13.33% and 30.77%, in compare with the close-ended circular pile and H-pile respectively. As their surface area and area of section is larger, the bearing capacity developed. The skin friction of pile increased as a result, with the close-ended square pile (Qu) showing the highest value among the other piles.

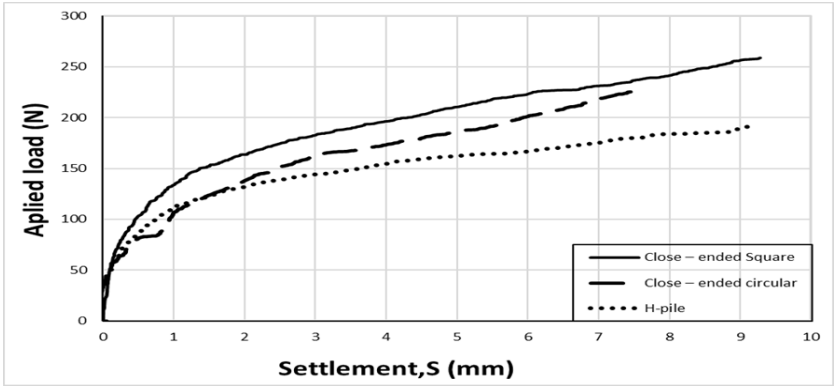

Fig 14. Load- settlement curves for different pile shapes at α=45° with L/D = 11.

Ultimate Pile Capacity for L/D ratio=14

Different shapes of piles have been employed to display the bearing capacity of pile. Figure 15 illustrates that the H-pile showed a higher displacement and minimal resistance. When compared values of Qu for close-ended square piles with H-piles have grown by 27.66%, and when compared to close-ended circular piles, they have increased by 9.1%.

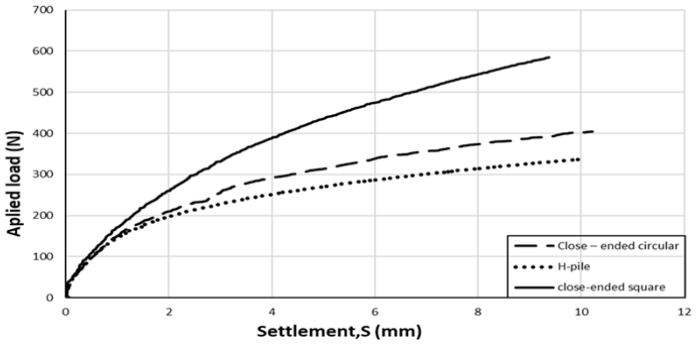

Fig. 15. Load- settlement curves for different pile shapes at α=45° with L/D = 14.

Ultimate Pile Capacity for L/D ratio=17

A static load test was utilized to ascertain the ultimate bearing capacity (Qu) of the piles. In Figure 16, the load-settlement curves for all pile types are displayed. When compared to the closed-ended circular and H-pile, the closed-ended square pile's carrying capacity is higher by 16.67% and 25%, respectively.

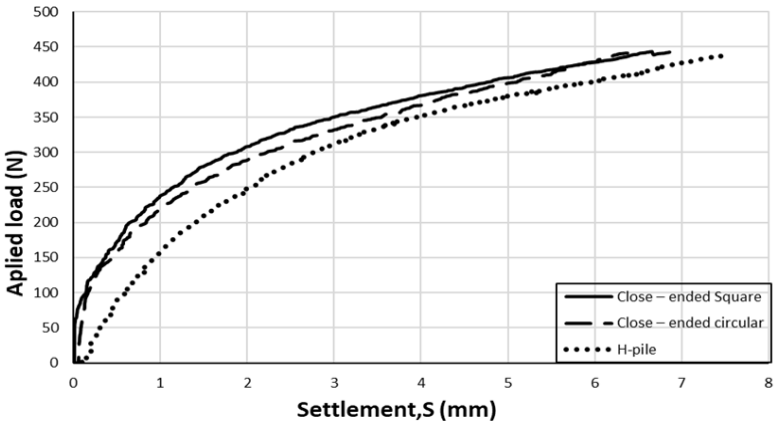

Fig 16. Load -settlement curves for different pile shapes at α=45° with L/D = 17.

The ultimate bearing capacity of piles placed under inclined loads at α=45° is summarized in Table 5.

TABLE 5. The pile's bearing capacity at α=45°

L/D	Pile shape	Qu(N)
11	Close – ended Square	170
	Close – ended circular	150
	H-pile	130
14	Close – ended Square	300
	Close – ended circular	275
	H-pile	235
17	Close – ended Square	350
	Close – ended circular	300
	H-pile	280

Inclined Load Tests at α=60°

In every type of pile utilized in the search, when the piles are subjected to an inclined load at α=60°, the vertical displacement becomes very low and the model fails with horizontal displacement.

Ultimate Pile Capacity for L/D ratio=11

Figure 17 shows the load-displacement curves for different types of piles when the inclined load of 60° with vertical was used to calculate the values of the ultimate bearing capacity of pile. All piles failed in horizontal displacement in this group of tests. It is clear that H-pile settlements were valued higher than settlements in other types of piles. Compared to the close-ended circular pile and H-pile, the results show that the close-ended square pile (Qu) values increased by 10% and 32%, respectively. Their ultimate capacity increased with their surface area and pile base. The result was increased the end bearing, with the close-ended square pile (Qu) indicating a higher value than the other piles.

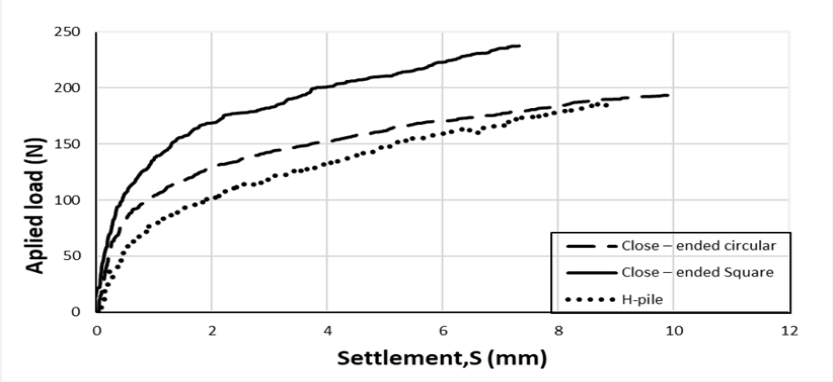

Fig 17. Load- settlement curves for different pile shapes at α=60° with L/D = 11.

Ultimate Pile Capacity for L/D ratio=14

Different shapes of piles have been utilized to show their Qu. The H-pile, shown in Figure 18, provided a higher lateral settlement with minimal resistance. Moreover, close-ended square pile Qu values have increased by 9.43% compared to close-ended circular piles and by 26.1% compared to H-piles.

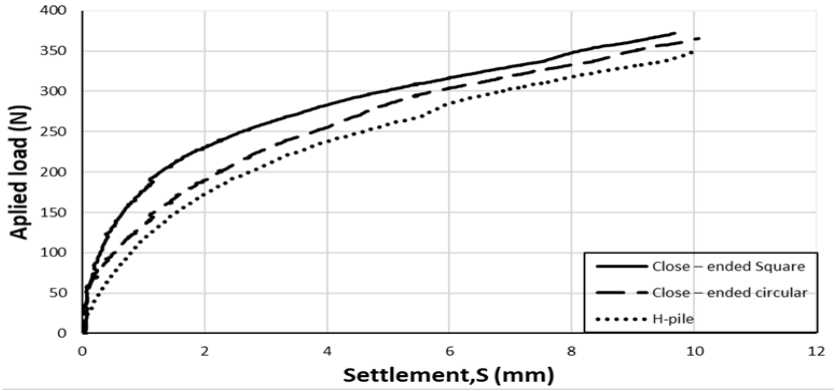

Fig. 18. Load -settlement curves for different pile shapes at α=60° with L/D = 14.

Ultimate Pile Capacity for L/D ratio=17

A static load test was used to determine the value of the piles' ultimate bearing capacity (Qu). For each type of pile, the load-settlement curves are shown in Figure 19. Whereas the carrying capacity of the closed-ended square pile is 19.23% higher than that of the H-pile and 8.8% higher than the closed-ended circular pile.

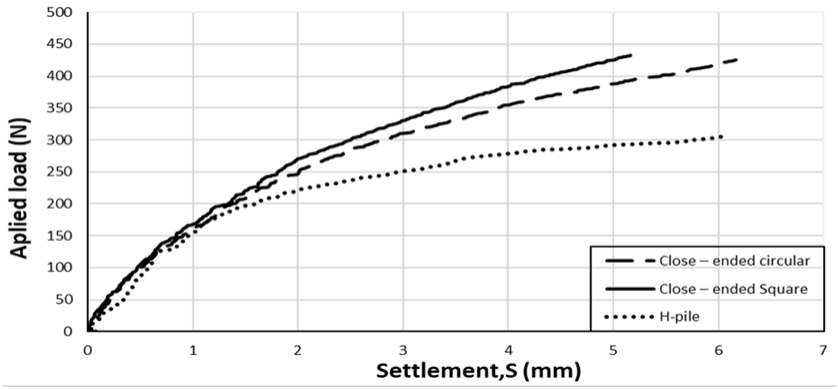

Fig 19. Load settlement curves for different pile shapes at α=60° with L/D = 17.

Table 6 gives a summary of the (Qu) of piles subjected to inclined loads at α = 60°.

TABLE 6. The pile's bearing capacity at α=60°

L/D	Pile shape	Qu(N)
11	Close – ended Square	165
	Close – ended circular	150
	H-pile	125
14	Close – ended Square	290
	Close – ended circular	265
	H-pile	230
17	Close – ended Square	310
	Close – ended circular	285
	H-pile	260

8 EFFECT OF PILE LENGTH

The effect of pile length on vertical and inclined load capability of pile was investigated by testing all model piles of different lengths with a constant pile diameter. With slenderness ratios of 11, 14, and 17, Figures 20, 21, 22, and 23 show how pile length affects a pile's capacity for vertical and inclined loads. It is evident from the results that as the pile lengthens, so its capacity to support vertical and inclined loads developed. This is because the surface friction increases as the embedment length of the pile increases.

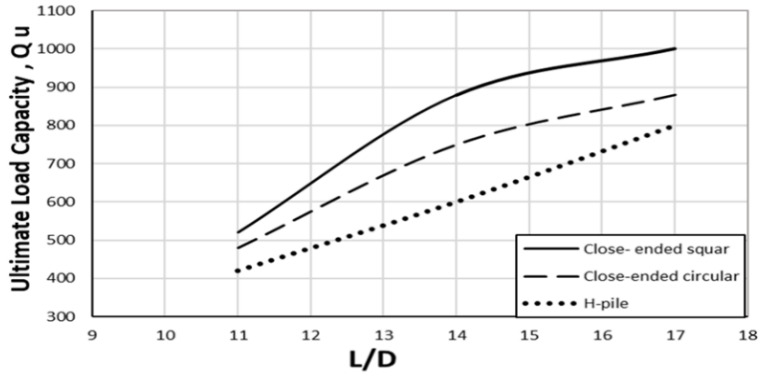

Fig. 20. Slenderness ratio versus Qu at vertical load.

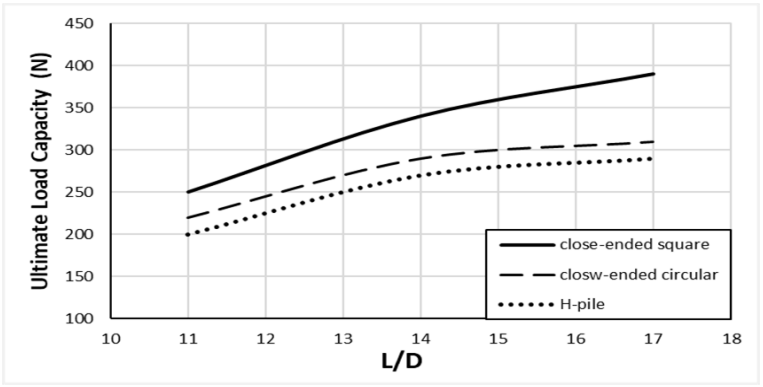

Fig 21. Slenderness ratio versus Qu at α=30°

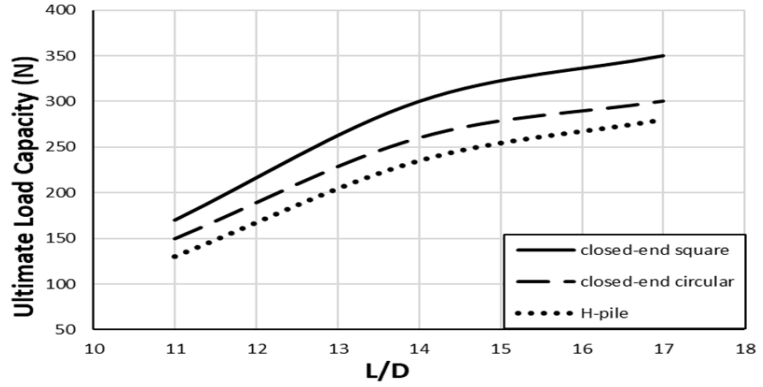

Fig 22. Slenderness ratio versus Qu at α=45°.

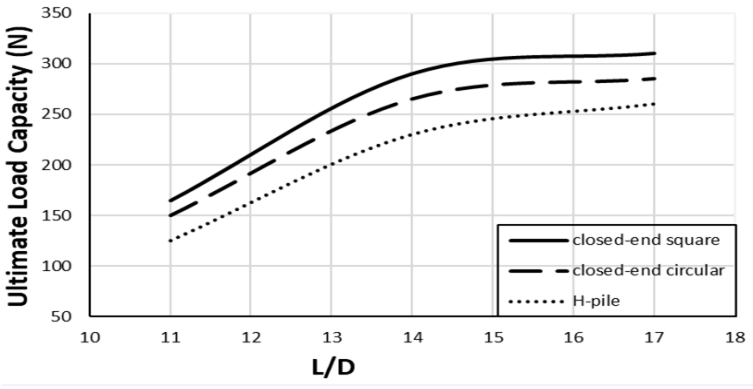

Fig 23. Slenderness ratio versus Qu at α = 60°.

9 EFFECT OF LOAD DIRECTION

One significant factor that affects the ultimate capacity of pile is the direction of the load. When loading was axial and inclined, different results were obtained. Test results show that the angle of the applied load has a major effect on the pile's ultimate capacity. The units have been transformed into dimensionless forms in order to remove the units, which makes the investigation more general, and enable it to be applied to different pile sizes. The symbol (F) utilized in this study is defined as failure load divided by the soil unit weight times the cubic pile length which is represented as dimensionless form by the symbol (F). Figures 24, 25, and 26 show the relationship between the load direction α and the form F. When comparing the vertical failure load and the subsequent failure load for different load inclinations, it is evident that for all piles, the form F decreases with increasing the load direction α.

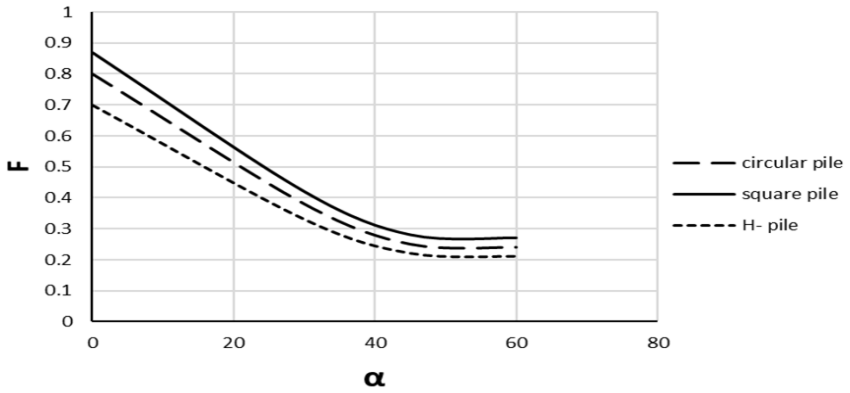

Fig. 24. Variation of F versus angles of load for L/D=11

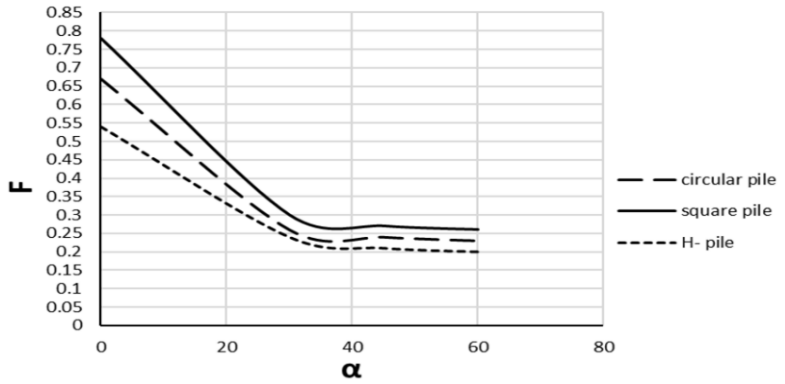

Fig. 25. Variation of F versus angles of load for L/D=14

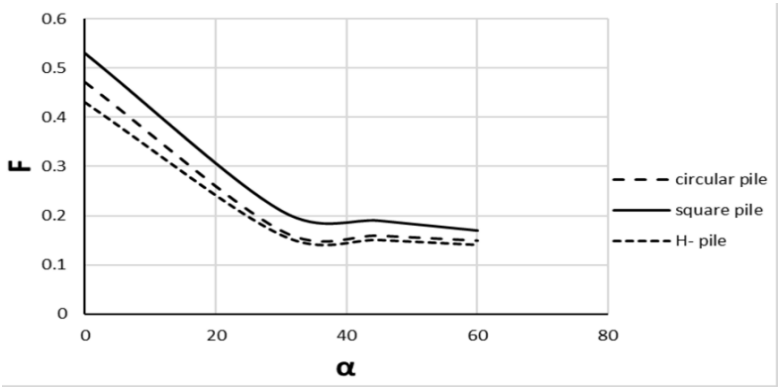

Fig. 26. Variation of F versus angles of load for L/D=17

10 CONCLUSIONS

The overall behavior of a single pile in sandy soil under vertical and inclined load was investigated in this study using the findings of the experimental tests. Based on the findings of the model pile tests, the following conclusions are presented:

- As the applied load's inclination with respect to the vertical (α) increased, the ultimate loads decreased.
- The ultimate capacity of piles embedded in sandy soil and subjected to vertical or inclined loads increases significantly as the slenderness ratio of pile (L/D) rises.
- The lateral displacement will increase as the applied load's inclination angle increases with vertical.
- The piles fail with horizontal displacement if they are subjected to an inclined load of more than 30.
- The largest ultimate bearing capacity among the other piles is shown in the squared piles.

REFERENCES

1. B. B. BROMS, “Lateral resistance of piles in cohesionless soils,” ASCE Journal of the Soil Mechanics and Foundations Division, 90(SM3): 123-1 56, 1964a.

2. B. B. BROMS, "Lateral resistance of piles in cohesive soils," ASCE Journal of the Soil Mechanics and Foundations Division, 90(SM2): 27-63, 1964b.
3. T. R. CHARI, and G. G. MEYERHOF, "Ultimate capacity of rigid single piles under inclined loads in sand," Canadian Geotechnical Journal, 20: 849-854, 1983.
4. G. G. MEYERHOF and V. V. R. N. SASTRY, "Bearing capacity of rigid piles under eccentric and inclined loads," Canadian Geotechnical Journal, 22: 267-276, 1985
5. G. G. Meyerhof and V. V. R. N. Sastry, "Full-displacement pressuremeter method for rigid piles under lateral loads and moments," Canadian Geotechnical Journal 24.4: 471-478, 1987.
6. V. V. R. N. SASTRY and G. G. MEYERHOF, "Lateral soil pressures and displacements of rig!d piles in homogeneous soils under eccentric and inclined loads," Canadian Geotechnical Journal, 23: 281-286, 1986.
7. H. G. Poulos, and E. H. Davis, "Pile foundation analysis and design" (Vol. 397). New York: Wiley, 1980.
8. G. G. Meyerhof and G. Ranjan, "The bearing capacity of rigid piles under inclined loads in sand. I: Vertical piles," Canadian Geotechnical Journal 9.4: 430-446, 1972.
9. E. Conte, L. Pugliese, A. Troncone, M. Vena, "A Simple Approach for Evaluating the Bearing Capacity of Piles Subjected to Inclined Loads," International Journal of Geomechanics, 21(11):04021224-. doi: 10.1061/(ASCE)GM.1943-5622.0002215, 2021.
10. S. M. Chirlam Charla, T. Munaga, and K. K. Gonavaram, "Influence of Inclined Loads on the Behaviour of Piles—A Numerical Study," Indian Geotechnical Conference. Singapore: Springer Nature Singapore, 2021.
11. R. K. Kalthiya, J. Dave, and M. V. Shah, "Model Study on Single Pile Subjected to Axial and Inclined Load Embedded in Contaminated Soil," Indian Geotechnical Conference. Singapore: Springer Nature Singapore, 2021.
12. ASTM, D 2216 98, "Standard Test Method for Laboratory Determination of Water (Moisture) Content of Soil and Rock by mass", 2000.
13. ASTM D1556-07, "Standard Test Method for Density and Unit Weight of Soil In Place By The Sand-Cone Method".
14. ASTM D422, "Standard Test Method for Particle Size Analysis of Soils," American Society for Testing and Materials, 2000.
15. ASTM International - ASTM D698-07," Standard Test Methods for Laboratory Compaction Characteristics of Soil Using Standard Effort".
16. ASTM D3080, "Standard Test Method for Direct Shear Test of Soils under Consolidated Drained Conditions," Philadelphia, PA: American Society of Testing Materials, 2014.
17. ASTM D4254, "Standard Test Methods for Minimum Index Density and Unit Weight of Soils and Calculation of Relative Density," Philadelphia, PA: American Society of Testing Materials ,2014.
18. ASTM D854, "Standard Test Method for Specific Gravity of Soil Solids by Water Pycnometer," American Society for Testing and Materials, 2005.
19. M. D. Bolton, M. W. Gui, J. Garnier, J. F. Corte, G. Bagge, J. Laue, and R. Renzi, "Centrifuge cone penetration tests in sand," Géotechnique 49, no. 4: 543-552, 1999.
20. M. F. Al-Zrejawi, "Performance of Pile Foundations under Axial Loading for Cohesive Soil," M. Sc. thesis, University of Kufa, 2022.
21. ASTM D 4643-17. "Standard test method for determination of water content of soil and rock by microwave oven heating," 2017.
22. M. N. Som and S. C. Das, "Theory and practice of foundation design," PHI Learning Pvt. Ltd., 2003.
23. V. N. S. Murthy, "Geotechnical engineering: principles and practices of soil mechanics and foundation engineering," CRC press, 2002.